Materials Chemistry and Physics 139 (2013) 988–997

Contents lists available at SciVerse ScienceDirect

Materials Chemistry and Physics

journal homepage: www.elsevier.com/locate/matchemphys

Influences of hyperbranched poly(amide-ester) on the properties of poly(butylene succinate)

Mingtao Run, Jian Wang, Meng Yao, Lijie Guo, Hai-jun Wang, Xinwu Ba*

Key Laboratory of Chemical Biology of Hebei Province, College of Chemistry & Environmental Science, Hebei University, Baoding 071002, PR China

HIGHLIGHTS

- H-bonding was detected between PBS and HBP phases by FTIR.
- HBP serves partly as a nucleating agent for the crystallization of PBS.
- HBP plays a role of plasticizer for PBS.
- The blend with 10%HBP has abnormal larger complex viscosity.

ARTICLE INFO

Article history:
Received 28 March 2012
Received in revised form
6 February 2013
Accepted 25 February 2013

Keywords:
Polymers
Crystallisation
Fourier transform infrared spectroscopy (FTIR)
Mechanical testing

ABSTRACT

The polymer blends of hyperbranched poly(amide-ester) and poly(butylene succinate) (HBP/PBS) were prepared by melt-blending method. The molecular interaction within the blends, phase morphology, crystal morphology, mechanical, rheological and dynamic mechanical properties were investigated by using Fourier transform infrared spectroscopy (FTIR), scanning electron microscopy (SEM), tensile machine, polarized optical microscopy, rotational rheometer and dynamic mechanical analyzer (DMA), respectively. The results suggest that PBS and HBP have a certain compatibility at amorphous state. A certain number of H-bonding was detected between PBS and HBP phases and it influences the material properties. HBP not only serves partially as a nucleating agent for the crystallization of PBS but also plays a role of plasticizer for the rheology of PBS. The glass transition temperatures of the blends slightly decrease with increasing HBP content. The proper amount of HBP (4–6%) has a reinforcement effect on the PBS matrix at glassy state. However, the blend with 10%HBP content has an improved impact strength mainly due to the plasticization effect or H-bonding effect of HBP on PBS matrix. The storage modulus is increased with increasing HBP contents, and the loss modulus is much smaller than the storage modulus in each blend at glassy state. At rubbery state the storage modulus of different samples is independent of HBP content. The complex viscosity of the melt decreases with increasing HBP content; however, the blend with 10%HBP is a special sample because of its abnormal larger complex viscosity at low shear frequencies. In addition, the melt's elasticity behavior increases slightly with increasing HBP content.

1. Introduction

Poly(butylene succinate) (PBS) is an aliphatic polyester with a large number of methylene in molecules, so it has similar mechanical properties, good thermal stability with traditional plastics, such as polypropylene (PP) and polyethylene (PE). In addition, compared to the biodegradable plastics, such as poly(-lactic acid), polyhydroxyalkanoates and polycaprolactone, PBS has good biodegradable properties, relatively cheap price and good processing property, so it is one of the focus of many industries and researchers [1,2]. However, the high crystallinity of PBS makes it brittle at room temperature [3], and its molding processing property is difficult to meet a variety of applications. Thus, preparing copolymer or blends is a preferred way for making PBS with better applications and performances [4,5].

Hyperbranched polymer (HBP) is an important branch in the field of polymer science [6]. In 1988, Kim and Webster [7,8] first synthesized a kind of HBP through the synthesis of soluble hyperbranched polyphenylene. HBP is a type of three-dimensional structure and highly branched polymer, which has excellent properties of dendritic polymers, such as high solubility, low viscosity, molecular chain nonentanglement and a large number of

* Corresponding author. Tel./fax: +86 312 5079317.
E-mail addresses: lhbx@hbu.cn (M. Run), baxw@hbu.cn (X. Ba).

0254-0584/$ – see front matter © 2013 Elsevier B.V. All rights reserved.
http://dx.doi.org/10.1016/j.matchemphys.2013.02.068

end groups. Recently, the synthesis and applications of HBP have attained more and more attentions due to its unique structure and properties [9]. Kim [10], Yan [11,12] and others [9,13,14] have done a lot of work in the synthetic HBP and its applications in some areas.

When HBPs are blended with other types of polymers, they can improve some of the performance of them [15–17]. Massa et al. [18] studied the blends of hyperbranched polyester and the linear polymer (such as linear polycarbonate, polyester and polyamide) and found that the polymer molecular structure and strong hydrogen bonding interaction determined the blend compatibility and phase behavior, and the blends of HBP/PC showed increasing tensile strength and compressive modulus. Kim et al. [10] found that the blends of hyperbranched polyphenylene and polystyrene showed lower viscosity and better thermal stability than that of pure polystyrene at high shear rates and high temperatures. Monticelle et al. [19,20] investigated the blends of aromatic polyamide type HBP and PA6 and found that the blend melt was shown mainly with elastic behavior, and a large number of functional groups in HBP were helpful for improving the compatibility of linear PA6 and HBP due to the covalent bond between HBP and PA6 or strong physical interactions (e.g. the hydrogen bonds), which led to nearly fully compatible of them. Månson et al. [21] studied the rheological properties of hyperbranched polyester (HBP-G2) on PET and found that the complex viscosity of blends decreased rapidly when HBP at the low concentration and HBP played a lubricant role. Bhardwaj et al. [22] studied the blends of PLA and HBP with cross-linking reaction. Zhang et al. [23] reported the mechanical and crystallization properties of the blends of a tree type HBP (DHP) and PLA. Xie et al. [24] found that the phase morphology of poly(methyl methacrylate)/polyurethane (HBP) blends was affected by the composition of HBP. Shi et al. [25,26] used hyperbranched poly(-amino acrylate) (HUA) to toughen PP. Yan et al. [27] characterized the blends of the linear polyphenylene sulfide (PPS)/hyperbranched polyphenylene sulfide (HPPS) and found that no phase separation in blends. With the increasing HPPS contents, the different blends showed a gradually increased single T_g, a decreased crystallinity, and an increased loss modulus and storage modulus. Zhu et al. [28] studied the amphiphilic star-hyperbranched polyester that was grafted to porous membrane of blends of polyethylene glycol (methyl-terminated) (HPE-MPEG) and PVDF, and found that HPE-MPEG could reduce the crystallinity of PVDF, improve porosity, and increase the temperature conductivity. Li et al. [29] found that with adding 2.5%HBP (poly(ester-amide)) in PLA, the viscosity of the PLA can be reduced by 40%. The hydrogen bonds between HBP and PLA proved by FTIR were increased with increasing HBP content.

In this work, in order to further investigate the influences of HBP on linear polymers, a series of blends composed of the hyperbranched poly(amide-ester) and PBS were prepared, and their phase morphology, thermal, mechanical and rheological properties, etc. were studied in detail. The results suggest that HBP plays polyroles on the properties of PBS, such as heterogeneous nucleating agent, plasticizer, and so on. Hydrogen bonds between HBP and PBS can be detected by FTIR and it can possibly induce abnormal performance of the blends.

2. Experimental

2.1. Raw material

Poly(butylene succinate) (PBS) powder was a commercial grade (HX-E101, Anqing Hexing Chemical Co., Ltd, China) with relative density of 1.26 g cm^{-3}. Hyperbranched poly(amide-ester) (HBP) was synthesized in our lab by succinic anhydride and diethanolamine according to Ref. [30]. HBP is viscous, soluble in water and cannot be made into solid spline. Some properties of PBS and HBP are listed in Table 1.

2.2. Blend preparation

HBP was dissolved in ethanol and then premixed together with PBS powders in high-speed mixer with different weight ratios of HBP/PBS as follows: 0/100, 2/98, 4/96, 6/94 and 10/90, and then dried in a vacuum oven for 2 h at 80 °C. The premixed blend was melt-blended in a self-wiping, co-rotating twin-screw, cone-shaped microextruder (SJSZ-5, Wuhan Ruiming Machinery, China), and the extrusion temperature in each section was controlled at 90, 135, and 135 °C. The resultant blend ribbons were cooled in cold water, cut into pellets, redried before being used in measurements.

2.3. Characterization

2.3.1. Differential scanning calorimetry characterization

The thermal properties measurements were performed on a differential scanning calorimetry (Perkin–Elmer Diamond DSC, USA) instrument under N_2 atmosphere with a flow rate of 20 mL min^{-1}. The as-extruded samples were heated from room temperature to 135 °C at a rate of 100 °C min^{-1}, held for 5 min to reset previous thermal history, then immediately quenched to −50 °C at a rate of 100 °C min^{-1}, held for 5 min; then heated again to 135 °C at a rate of 10 °C min^{-1}, held for 5 min, and finally cooled to −50 °C at a rate of 10 °C min^{-1}; the final heating and cooling processes were recorded.

The isothermal crystallization behaviors were measured by the following steps: the dried sample was heated from room temperature to 130 °C at a heating rate of 50 °C min^{-1} under N_2 atmosphere, held for 5 min, and then cooled down rapidly to the specified temperature (T_c) at a cooling rate of 100 °C min^{-1}, held for 20 min for the completion of the crystallization. T_c was set as 96, 98, 100, 102, and 104 °C, respectively. Then the crystalline samples were heated to 130 °C at a heating rate of 10 °C min^{-1}. The isothermal crystallization process and subsequent melting process were recorded.

2.3.2. Characterization of crystal morphology

The crystal morphology was studied by using a polarized optical microscopy (BX-51, Olympus, Japan). The samples were first melted between two glass slides on a hot stage at 130 °C for 5 min, pressed into a film, then cooled to the temperature at a rate of 1 °C min^{-1} until the nuclei formed, held at this temperature for 4 h and then taken photographs.

2.3.3. Characterization of mechanical properties

The blend pellets were made into the standard splines using a microinjection molding machine (SZ-15, Wuhan Ruiming Machinery, China). The impact strength was measured with an impact tester (JJ-5.5 type, Changchun Intelligent Instrument Co., Ltd.) according to ISO179-1982. Tensile strength testing was performed with a universal testing machine (WSM-20, Changchun Intelligent Instrument Co., Ltd.) with a crosshead speed of 10 mm min^{-1} at room temperature (25 °C) according to the GB/T16421-1996. The dimensions of the dumbbell-shaped specimen for testing are shown in the Appendix file Chart 1.

Table 1
The properties of PBS and HBP sample.

Sample	M_z	M_n	M_w	T_g (°C)	T_m (°C)
PBS	20,000	–	–	−29.4	115
HBP	–	4200	54,000	−28.4	–

2.3.4. Phase morphological characterization

The phase morphology was observed by using the KYKY-2800B type scanning electron microscopy (SEM, KYKY Technology Development Ltd., China). In order to etch the HBP component from the PBS matrix, the samples with the fracture surface prepared in the impact testing were immersed in deionized water for 5 h, and then they were dried and sprayed gold, observed by the SEM at a voltage of 25 kV.

2.3.5. Characterization of rheological behavior

For studying the rheological behavior, the sample was pressed into a wafer with the diameter of 25 mm and the thickness of 1.1 mm at 135 °C. The rheology measurements were carried out on a rotating rheometer (AR2000ex, Waters-TA Co., USA). Frequencies sweep for the samples was carried out under N_2 at 125 °C using 25 mm plate-plate geometry with plate spacing of 1.0 mm. The strain and frequency range used during testing were 1% and 0.628–628 rad s^{-1}.

2.3.6. Dynamic mechanical analysis

Dynamic mechanical property testing was performed on a dynamic mechanical analyzer (DMA8000, Perkin-Elmer, USA). The spline with size of 10 × 5 × 2 mm was prepared by injection molding. The temperature range was from −80 to 80 °C with a heating rate of 3 °C min^{-1} and a frequency of 1 Hz.

2.3.7. FTIR spectroscopy analysis

FTIR spectra were recorded with a Varian-640 spectrophotometer (KBr pellet technique) in the wavenumbers from 2000 to 1550 cm^{-1} with a resolution of 1 cm^{-1} and averaged over 40 scans.

3. Results and discussion

3.1. Infrared spectroscopy analysis

Fig. 1 shows the FTIR spectra for pure PBS and its blends with various HBP contents. In Fig. 1, two new absorption bands near 1625 and 1560 cm^{-1} appear and their absorption intensity become stronger and stronger with increasing HBP content. They belong to the vibrations of the acylamide group (CONH) in HBP. Remarkably, the absorption peak of the strong C═O ester carbonyl stretch vibration of PBS is around the range of 1750–1725 cm^{-1}. As known, when the C═O forms hydrogen bonding (H-bonding) with other atoms, such as H of the hydroxyls −OH, the absorption peak of ester carbonyl will split into two bands, and the peak at larger wavenumber should be the characteristic of the free ester carbonyl stretching mode, while the peak at lower wavenumber should be the characteristic of hydrogen bonded (H-bonded) carbonyl [31]. For pure PBS, it has end-groups of hydroxyls (−OH) and ester carbonyl (C═O), thus some H-bonding between −OH and C═O will form intermolecular chains. As shown in Fig. 1, the FTIR curve of the PBS showed the vibrations of both free C═O and H-bonded C═O. As shown in Scheme 1, when the PBS was melt-blended with HBP, some H-bondings will form between the end-groups of HBP (−OH) and the ester carbonyl of PBS (C═O). Therefore, no new type H-bonding formed in the blends and as a result, no new vibration peak appears in the FTIR curve of each blend. Although there are no new vibrations appearing in the blend's curve, the changes of the peak intensities of corresponding bands of the groups were observed in Fig. 1. As seen in Fig. 1, for each sample of the pure PBS and the blends with 2%HBP and 4%HBP, the vibration peak of H-bonded C═O had nearly equal intensity with that of free C═O; this maybe because of their low content of HBP and little increased amounts of H-bonded C═O between PBS and HBP; however, in each sample of the blends with 6%HBP and 10%HBP, the vibration peak of H-bonded C═O had a clear larger intensity than that of free C═O, indicating that when the HBP content increased to proper content, the amounts of hydrogen bonds formed in the blends were more and more, and the increasing intensity of the H-bonded C═O peak was due to the increasing H-bonding between PBS and HBP.

The fraction of the H-bonded carbonyl group can be calculated by the following equation:

$$f_b^{C=O} = \frac{A_b/1.5}{A_b/1.5 + A_f} \quad (1)$$

where A_f and A_b are peak areas corresponding to the free and H-bonded carbonyl groups, respectively. The conversion coefficient 1.5 is the ratio of these two bands in an ester group [31]. The curve fitting results are summarized in Table 2. These results in Table 2 suggest that the H-bonded C═O increases with increasing HBP content, indicating that the amount of hydrogen bonds is increased

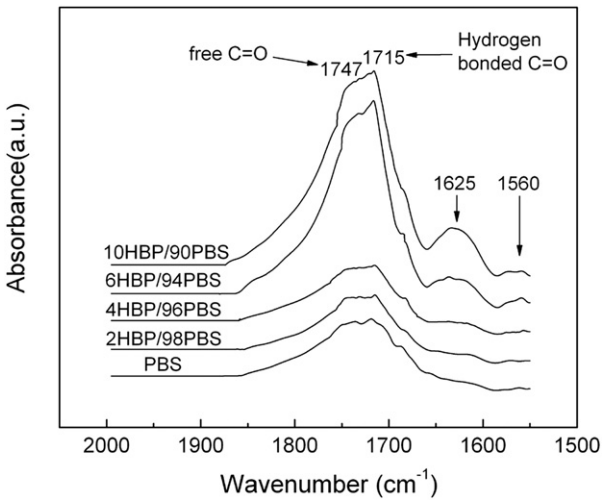

Fig. 1. FTIR of PBS and HBP/PBS blends.

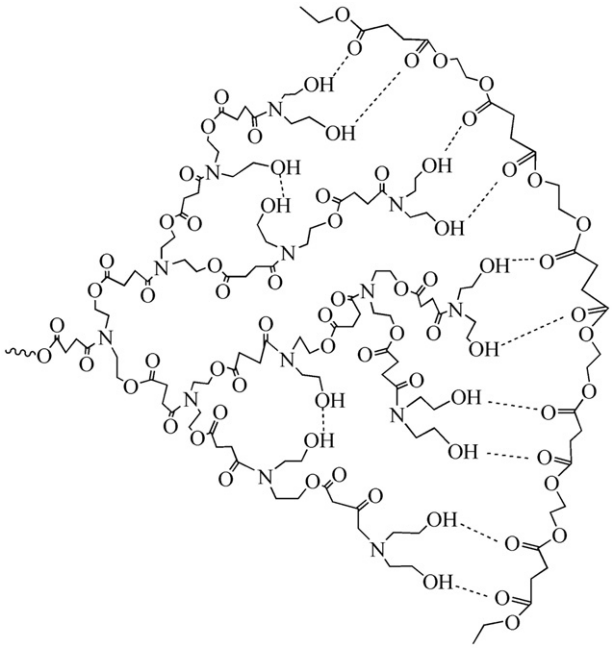

Scheme 1. Schematic illustration of intermolecular H-bonding between HBP and PBS.

Table 2
Fraction of the H-bonded and free carbonyl group in the blends.

HBP/PBS	H-bonded C=O			Free C=O			f_b (%)
	ν (cm^{-1})	$W_{1/2}$[a] (cm^{-1})	A_b (%)	ν (cm^{-1})	$W_{1/2}$[a] (cm^{-1})	A_f (%)	
0/100	1718.7	44.0	21.8	1747.2	90.7	78.2	15.7
2/98	1717.2	50.0	29.5	1747.3	87.7	70.5	21.8
4/96	1716.7	47.9	34.2	1746.9	86.0	65.8	25.7
6/94	1716.2	34.9	35.8	1743.5	61.5	64.2	27.1
10/90	1716.2	39.2	39.3	1743.9	60.9	60.7	31.2

[a] Peak-width at half peak-height.

in blends as the hydroxyl groups increase in blends. The FTIR technique is useful to verify this specific interaction between polymers because of its sensitivity to H-bonding formation.

Scheme 1 gives a schematic illustration of intermolecular hydrogen bonding between HBP and PBS. The abundance of terminal −OH groups of HBP provides a favorable condition for the formation of hydrogen bonds. As shown in Scheme 1, the H-bonding involves C=O groups of PBS often regarded as H-bonding acceptor, and −OH of HBP usually regarded as H-bonding donor. On the other hand, the H-bonding in the blend also involves the strong hydrogen bonding between −OHs of HBP (as shown in Scheme 1). Thus, it may be deduced that the compatibility between PBS and HBP in the blends will be enhanced due to the H-bonding [32], although they are different between the molecular structure and polarity. Furthermore, we believe that the intermolecular H-bonding will influence the mechanical, rheology, glass transition and dynamic mechanical properties of the blends.

3.2. Characterization of crystal morphology

Fig. 2 shows the polarizing optical microscopy (POM) photographs of different samples. The crystal morphology of PBS is the spherulite for the photograph in Fig. 2(a) is shown with Maltese-cross extinction patterns. As seen in Fig. 2(b)–(e), the spherulite size becomes smaller and smaller with increasing HBP content, especially in Fig. 2(e) nearly no perfect spherulites can be observed clearly. Firstly, HBP is an amorphous phase and it can be served as heterogeneous nucleating agent for PBS, so the nucleation density increases as HBP content increases, which leads to smaller size or even imperfect crystals. Secondly, HBP component influences the molecular interactions (e.g. H-bonding) and molecular mobility of PBS, thus the arrangement of PBS molecules is changed, and the crystal morphology is changed as well. So, it can be deduced from the above results that the mechanical property should be

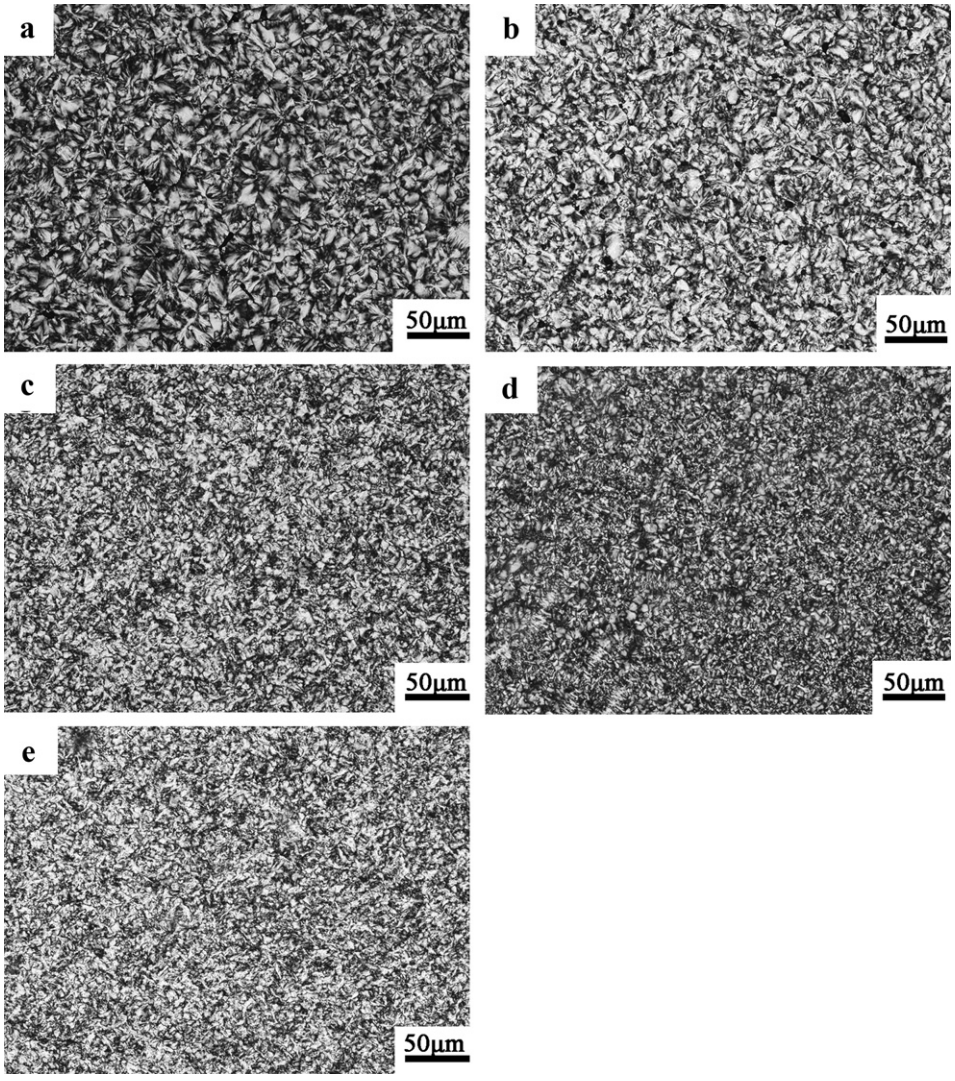

Fig. 2. POM photographs of the different crystalline blends. (a) PBS, (b) 2HBP/98PBS, (c) 4HBP/96PBS, (d) 6HBP/94PBS, (e) 10HBP/90PBS.

improved by the HBP because of the microcrystallites formed in the blends.

3.3. Mechanical properties

Because molecular entanglements are absent in the HBP, the material obtained from neat HBP is unable to make standard spline for testing. Fig. 3 shows the tensile strength and elastic modulus of different samples, and the data are listed in Table 3. In Fig. 3, the tensile strength and elastic modulus first increase and then decrease with increasing HBP content, in which they reach the maximum values with HBP content of 6%. These results suggest that the proper content of HBP in PBS matrix plays a role in improving the tensile strength and modulus although its effect is not so obvious. This result can also be deduced from the results in Fig. 2 and the H-bonding interaction in Table 2, that is to say, the microcrystallites of PBS and H-bonding interaction between HBP and PBS are both favorable to improve the tensile strength of the blend. However, the tensile strength decreases when HBP content is 10%. We know that HBP has a much lower strength than PBS and it has a dilution effect on PBS matrix. Thus, in the blend of 10HBP/90PBS, as HBP content increases to a critical content, the above two negative effects become dominant on the tensile strength and they suppress the H-bonding interaction effect and microcrystallite effect; consequently, the tensile strength of the blend is deteriorated. In a word, all the contributions to tensile strength summed together explained well why an optimum in tensile strength was observed using proper concentration of HBP.

The impact strength data of PBS and the blends are listed in Table 3. The impact strength of PBS is the largest in all the samples. When HBP contents are in the range of 2–6%, the impact strength of three blends is about 7.0 kJ m^{-2}. This result maybe mainly induced by the weak impact strength of HBP. However, the impact strength of the blend with HBP content of 10% is 8.6 kJ m^{-2}, which maybe induced by the plasticization effect of HBP and/or the larger H-bonding interaction effect (see f_b in Table 2).

3.4. Phase morphology

Fig. 4 shows the SEM images of the fracture surface of different blends. As shown in Fig. 4(A), when HBP content is 2%, a few small spherical cavities are observed in the fracture surface. As seen in images B, C and D, when HBP content increases from 4% to 10%, not only the number but also the size of the cavities are both increased, indicating that the dispersed phase of HBP is uniformly formed in the blends and they gather together into aggregation with diameter from several microns to about ten microns. As we know, the H-bonding formed between hydroxyl of HBP and carbonyl of PBS can increase the interface adhesion, thus a uniform dispersion of cavities can be observed in the surface, especially in Fig. 4(C). However, several large cavities are observed in those blends with high HBP contents. It is because of not only their difference in structure and polarity, but also not all of the hydroxyl groups in HBP are involved in hydrogen bonds between PBS and HBP. As HBP content increases, the hydroxyl groups prone to interact with themselves due to the stronger intramolecular hydroxyl–hydroxyl bonds than the weak intermolecular hydroxyl–carbonyl bonds, which leads to the aggregation of HBP. Therefore, the cavity diameter of HBP in blend increases with increasing HBP content. However, as seen in Fig. 4(C), the dispersion of HBP is uniform in the matrix and its average phase diameter is less than 4 μm, indicating that there is certain compatibility between them.

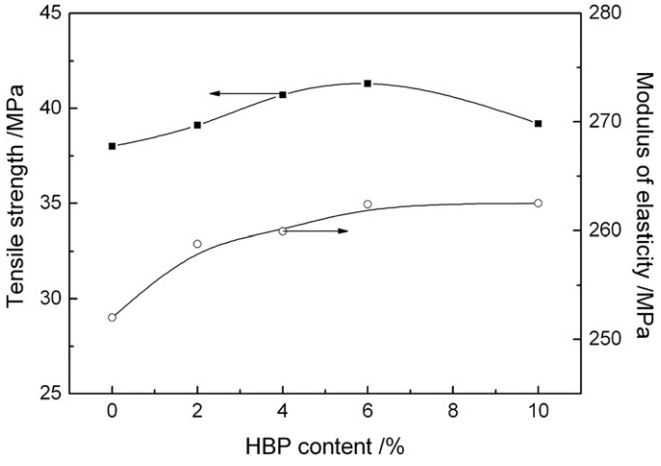

Fig. 3. Tensile strength and modulus of different samples.

Table 3
The mechanical properties of different samples.

Sample	Tensile strength (MPa)	Elastic modulus (MPa)	Impact strength (kJ m^{-2})
PBS	38.0	252.1	8.9
2HBP/98PBS	39.1	258.8	7.0
4HBP/96PBS	40.7	259.9	7.3
6HBP/94PBS	41.3	262.4	7.1
10HBP/90PBS	39.2	260.6	8.5

3.5. Melting and crystallization behavior

The compatibility of the blends can be characterized by measuring the T_g of the blends. Fig. 5 shows the DSC melting curves of the samples at a heating rate of 10 °C min^{-1} and the data are listed in Table 4. It can be seen that pure PBS and HBP have the close T_gs of −29.4 °C and −28.4 °C; and each blend also has a single T_g, which decreases slightly with increasing HBP content. The single T_g of each blend in Table 4 is mainly attributed to PBS phase because the concentration of HBP is relative low in blend and its transition maybe overlapped by the transition of PBS. The single and decreasing T_g of the blends indicates that PBS and HBP have some compatibility, which may be due to the H-bonding between HBP and PBS. The formation of hydrogen bonds usually induces the miscibility of the blends, as has been shown for many hydrogen-bonded blends [33]. Furthermore, a melting-recrystallization behavior can be observed in each DSC curve, and the recrystallization peak temperatures (T_{re}) are increased slightly with increasing HBP content, indicating that the recrystallization of PBS is influenced by molecular interactions between PBS and HBP phases. In addition, the melting points (T_m) of the blends are increased with increasing HBP content, suggesting that the crystal lamellas in blends formed after recrystallization are thicker than those in pure PBS; it may be the dilution effect of HBP that improves the molecular arrangement in the recrystallization process.

Fig. 6 shows the DSC melt-crystallization curves of PBS and the blends at a cooling rate of 10 °C min^{-1} and the parameters are listed in Table 4. The start crystallization temperature (T_{oc}) and crystallization peak temperature (T_{pc}) are both decreased with increasing HBP content. As HBP contents are 2–6%, their T_{oc} and T_{pc} of the blends are lower than that of pure PBS, therefore ΔT values and the full width at half-height of crystallization peak (FWHP) are both reduced with increasing HBP content. In addition, the ΔH_c values of the blends are also higher than that of pure PBS. Above results suggest that HBP can increase not only the crystallization rate but also the crystallinity of the blends. HBP acts as a nucleating agent

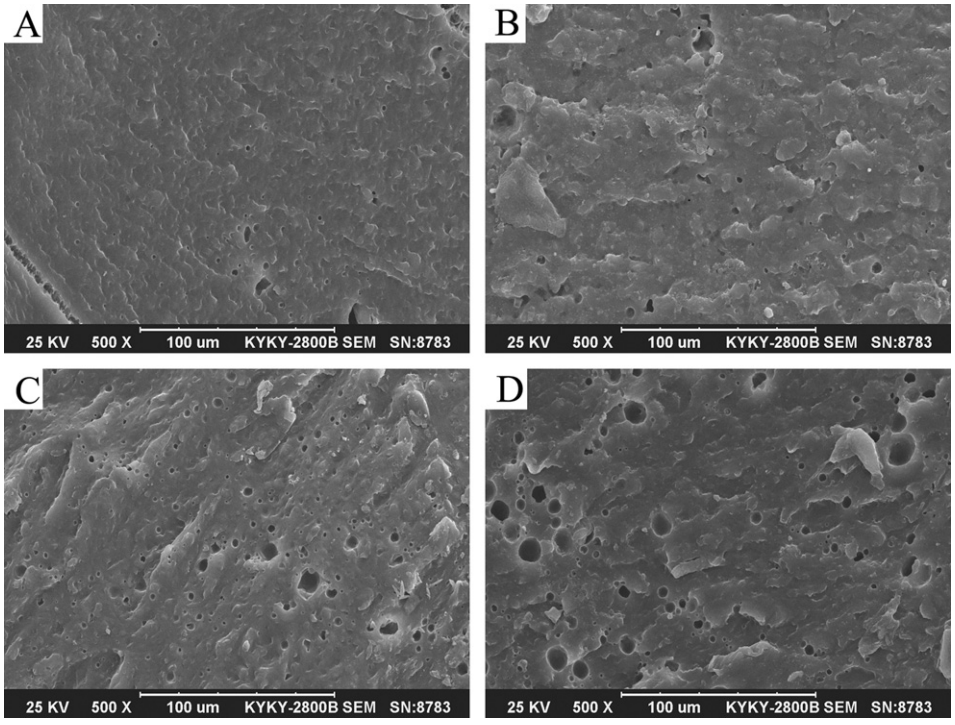

Fig. 4. SEM micrographs of PBS/HBP blends. (A) 2HBP/98PBS, (B) 4HBP/96PBS, (C) 6HBP/94PBS, (D) 10HBP/90PBS.

for the crystallization of PBS. This result is consistent with the blends' crystal morphology observed in Fig. 2. However, the blend with 10%HBP is a special sample because all of its parameters, such as T_{oc}, T_{pc}, ΔT, FWHM and ΔH_c, are not the least one among all the data, like other properties (the impact strength, the rheology behavior, etc.). These phenomena maybe induced by its larger H-bonding effect, which changes the former orderliness and endow with new performance on the blend.

3.6. Isothermal crystallization kinetics

Most PBS materials are prepared to final products by melt-injection molding process; therefore, the crystallization rate and kinetics are important properties of PBS. The PBS and the blend with 4%HBP was studied for their crystallization kinetics, and the specific temperatures (T_c) of isothermal crystallization experiment were 96–104 °C. Assuming that the relative crystallinity (X_t) increases with the crystallization time (t), the classical Avrami equation can be used to analyze the isothermal crystallization process of neat PBS and the blends as follows [34,35]:

$$X_t = 1 - \exp(-K_t t^n) \tag{2}$$

where X_t is the relative degree of crystallinity at time t; the exponent n is a mechanism constant depending on the type of nucleation and the growth dimension, and the parameter K_t is a growth rate constant involving both nucleation and the growth rate parameters. During the isothermal crystallization, heat flow (dH/dt) can be probed over crystallization time via DSC. One can derive the percent of ultimate crystallization vs. time by using Eq. (5) and applying it to the exothermic crystallization peak:

$$X_t = \frac{\int_{t_0}^{t} (dH/dt)dt}{\int_{t_0}^{t_\infty} (dH/dt)dt} = \frac{A_t}{A_\infty} \tag{3}$$

where the dH/dt is the rate of heat flow, t_0 and t_∞ are the times at which crystallization starts and ends, respectively; and A_t and A_∞ are areas under the normalized DSC curves at times t and the end of the crystallization, respectively.

Taking the double logarithm of Eq. (2) gives

$$\log[-\ln(1 - X_t)] = n \log t + \log K_t \tag{4}$$

where suggests that $\log[-\ln(1 - X_t)]$ vs. $\log t$ should be linear, and K_t and n can be calculated by fitting a line to the experimental data.

The plots of $\log[-\ln(1 - X_t)]$ vs. $\log t$ according to Eq. (4) are shown in Fig. 7. The parameters of n and $\log K_t$ of the primary

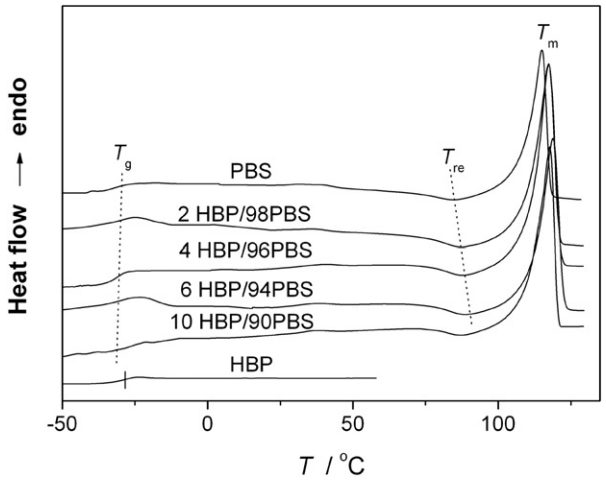

Fig. 5. DSC melting thermograms at the heating rate of 10 °C min^{-1}.

Table 4
DSC parameters during the melt-crystallization and subsequent melting process.

Sample	Melting process			Crystallization process				
	T_g (°C)	T_{rc} (°C)	T_m (°C)	T_{oc} (°C)	T_{pc} (°C)	$\Delta T = T_{oc} - T_{pc}$ (°C)	FWHP (°C)	ΔH_c[a] (J g^{-1})
PBS	−29.4	84.9	115.2	78.9	71.3	7.6	6.8	−50.0
98PBS/2HBP	−29.9	86.4	117.7	77.5	71.4	6.1	5.9	−64.9
96PBS/4HBP	−30.2	87.4	117.9	76.4	70.0	6.4	5.9	−64.8
94PBS/6HBP	−30.6	88.9	118.9	76.4	69.8	6.6	5.8	−66.1
90PBS/10HBP	−31.2	87.4	117.4	77.1	70.6	6.5	5.9	−67.8
HBP	−28.4		–	–	–	–	–	–

[a] Data are normalized for the percentage of PBS in the blend.

crystallization stage are obtained by the fitting line slope and intercept, and the half-crystallization time, $t_{1/2}$, can also be obtained by the following equation:

$$t_{1/2} = (\ln 2/K_t)^{1/n} \quad (5)$$

The isothermal crystallization kinetics parameters are listed in Table 5. For each sample, K_t decreases and $t_{1/2}$ increases with T_c increasing, indicating that crystal nucleation and growth rates are dependent on the crystallization temperature. Compared the K_t and $t_{1/2}$ values of PBS and the blend with 4%HBP at the same T_c, it can be found that the blend has larger K_t and lower $t_{1/2}$, indicating that HBP increases the crystallization rate of PBS. However, judging from the K_t values of the two samples, the nucleation role is relatively weak, so we believe that HBP partially plays a role of nucleating agent for PBS.

The Avrami exponent n of PBS is mainly around 4.0, suggesting that PBS tends to form spherulites at homogenous state. While for the blend with 4%HBP, n is lower than that of PBS at the same T_c, and they all tend to 3.0, suggesting that PBS also tends to form spherulites as HBP partially serves as heterogeneous nucleating agents for PBS. These results are consistent with the crystal morphology as shown in Fig. 2. The values of n are not an integer for all the samples, which may be due to the stack of crystals in the process of crystal growth. When the macromolecules crystallize from melting state, the molecular chains that do not produce large-scale diffusion and adjustment are different to the small molecules; in addition, the crystal growth dimension cannot be just an integer for the molecular chain entanglement.

3.7. Rheological behavior

The polymer blend with two or more components is a multiphase flow. The rheology of the flow has some connections with not only the frequency, temperature, etc., but also with the nature, content and mobility patterns of each component and so on. PBS and the blends are swept of frequency (0.628–628 rad s^{-1}) at 125 °C, receiving the curves of storage modulus (G'), loss modulus (G'') and complex viscosity (η^*) dependent on frequency, as shown in Figs. 8–10.

Fig. 8 shows the curves of η^* vs. ω of different samples. PBS has the largest η^* among all the samples; while for the blends with HBP content of 2%, 4% and 6%, η^* decreases gradually with increasing HBP content. Several factors might be responsible for the decreased melt viscosity. Firstly, it was reasonable to expect the globular-shaped hyperbranched polymers to destroy the copious entanglements of linear PBS chains. As a result, introducing HBP to PBS will result in fewer entanglements in the blend and HBP plays a role in isolation. Secondly, the free volume of the blend system will

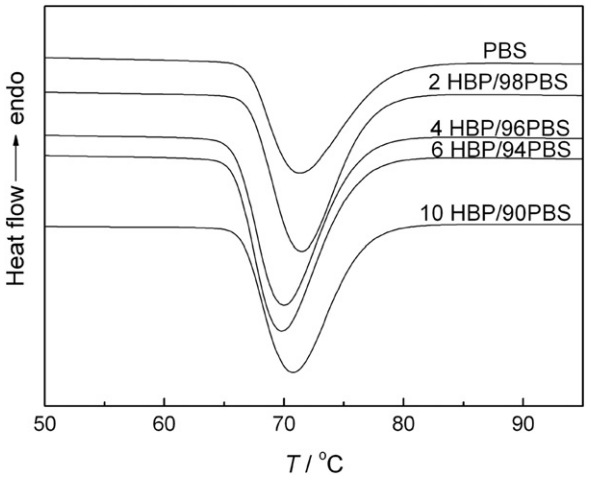

Fig. 6. DSC crystallization curves at the cooling rate of 10 °C min^{-1}.

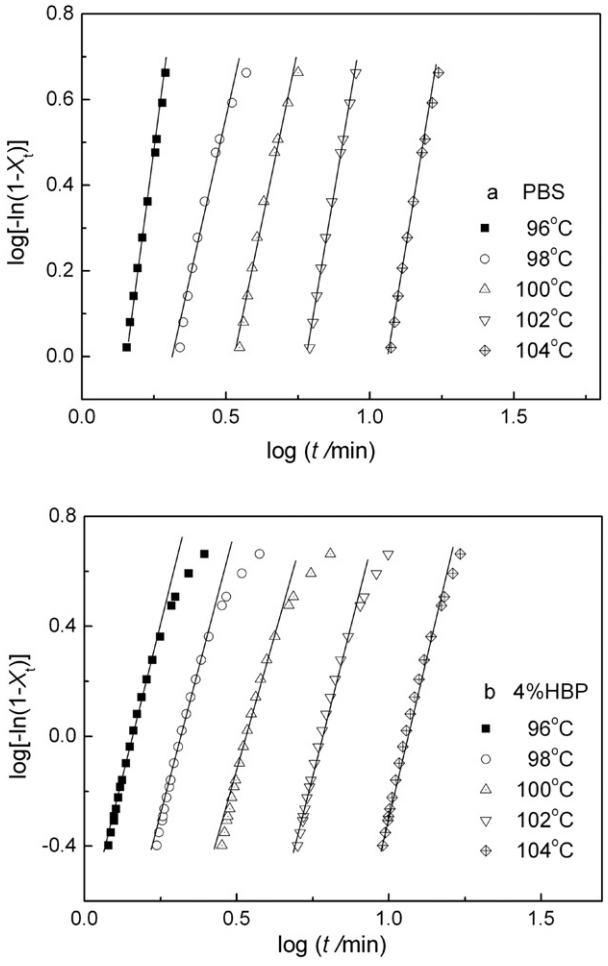

Fig. 7. Plots of log[−ln(1 − X_t)] vs. log t for (a) PBS and (b) 4%HBP blend.

Table 5
The isothermal crystallization kinetic parameters of PBS and 4%HBP blend analyzed by Avrami equation.

Sample	T_c (°C)	K_t	$t_{1/2}$ (min)	n
PBS	96	2.03×10^{-1}	1.33	4.6
	98	1.26×10^{-1}	2.00	2.8
	100	1.99×10^{-2}	3.25	3.2
	102	7.62×10^{-4}	5.70	3.9
	104	7.31×10^{-5}	10.96	3.9
96PBS/4HBP	96	2.48×10^{-1}	1.31	3.6
	98	7.60×10^{-2}	1.92	3.4
	100	1.73×10^{-2}	3.14	3.2
	102	1.12×10^{-3}	5.55	3.7
	104	3.08×10^{-5}	10.53	4.2

become larger with the addition of HBP due to its abundant end groups. With the increase of free volume, the internal friction of molecules is decreased, so the melt viscosity significantly decreases. Thirdly, it is the result of the large disparity between the intrinsic viscosity of PBS and HBP [29].

The blend with 10%HBP is a unique one here for its special rheology. In the low frequency range ($\omega < 10$ rad s^{-1}), the η^* of blend is lower than that of PBS but obviously larger than all the other blends; however, in the high frequency range ($\omega > 10$ rad s^{-1}), the η^* of the blend decreases rapidly to lower than that of all the other blends. Combining with the SEM images shown in Fig. 4(D), it is reasonable that with HBP content reaching 10%, the phase separation of HBP is more obvious. In the two-phase interface, the interaction between molecules of HBP and PBS (mainly H-bonding) leads to the η^* increasing. When the cumulative interactions reach a certain amount of value, it will depress the negative effect of HBP on η^*, and this blend will have a larger η^* than other blends when the frequency is low enough and cannot destroy the interactions between the molecules (e.g. H-bonding). However, when the frequency is high enough to destroy the interactions between the molecules, η^* will be declined with increasing frequencies and finally being lower than that of other blends.

Complex viscosity η^* can be decomposed into the G' and G''. The elastic part of η^* is described by the G' that shows the size of the recoverable energy stored in melting sample, while the viscous part is described by the G'' that shows the size of the non recoverable energy. Figs. 9 and 10 show the changes of G' and G'' with the frequency. In Fig. 9, when ω<100 rad s^{-1}, G' of the blends containing HBP of 2–6% is lower than that of PBS, while G' of the blend

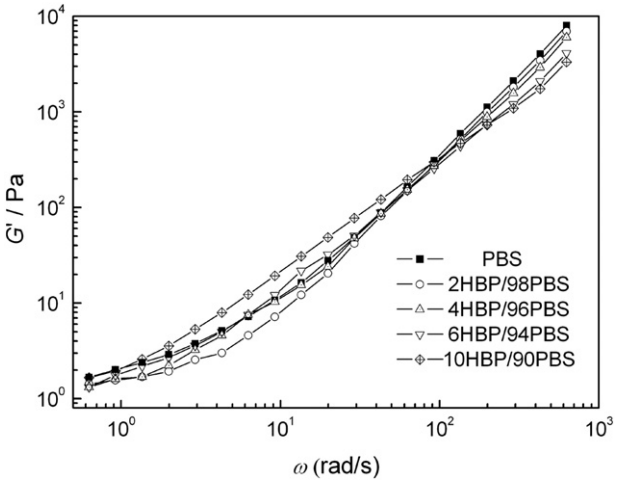

Fig. 9. Curves of G' vs. ω for different samples.

containing HBP of 10% is larger than that of PBS. When $\omega > 100$ rad s^{-1}, G' decreases regularly with increasing HBP content from 0% to 10%. The G'' of different blends is nearly similar as shown in Fig. 10, and it is decreased slightly with increasing HBP content.

In the low frequencies area, HBP has two different effects of dilution and adhesion on the PBS matrix: (1) When HBP content is lower than 6%, HBP plays a major role of dilution, and the storage modulus of the blend is decreased, so that G' for 2%HBP, 4%HBP, 6% HBP is lower than that of pure PBS. But G' increases gradually with increasing HBP content, indicating that the molecular interactions between PBS and HBP reduce the dilution effect of HBP; (2) When the HBP content is as high as 10%, HBP plays a main role of adhesion, and the reason for this effect could be related to the molecular interactions between PBS and HBP, i.e. hydrogen bonding effect, so its G' is larger than that of pure PBS.

In the high frequencies area, the dilution effect takes a major role because the molecular interactions between PBS and HBP are easily damaged by mechanical shearing, so G' shows a gradually decline with increasing HBP content.

Fig. 11 shows the plots of G' vs. G'' for different samples, which is termed as Cole–Cole plot. A Cole–Cole plot is useful for comparing the effect of different HBP compositions on rheological behavior of blends. As G'' is greater than G', it means that the melt's elastic behavior is less than viscous behavior. As seen in Fig. 11, all the

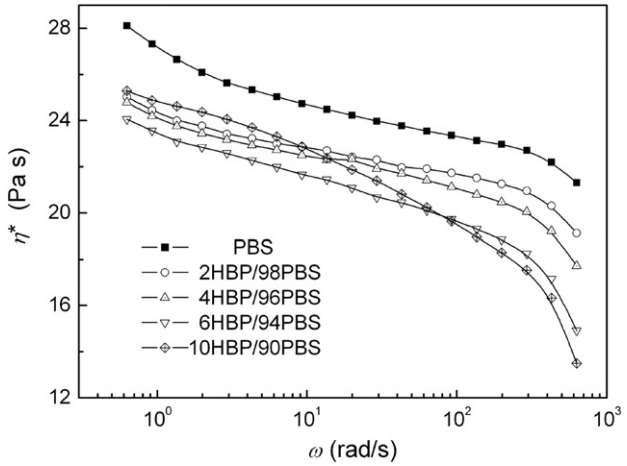

Fig. 8. Curves of η^* vs. ω for different samples.

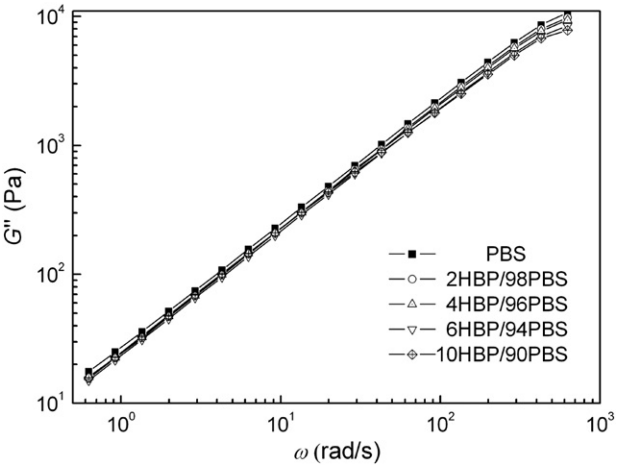

Fig. 10. Curves of G'' vs. ω for different samples.

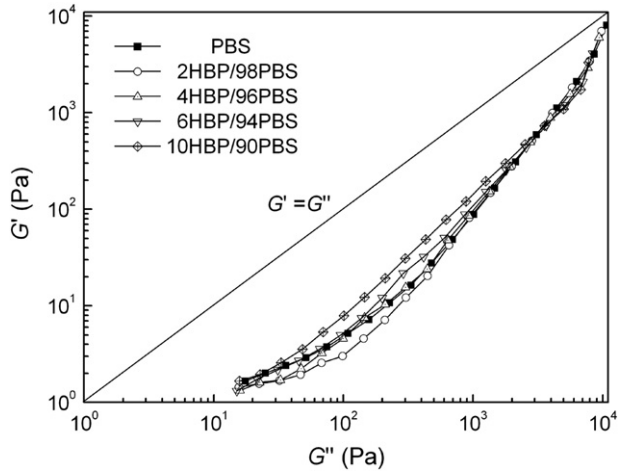

Fig. 11. Curves of G' vs. G'' for PBS/HBP blends.

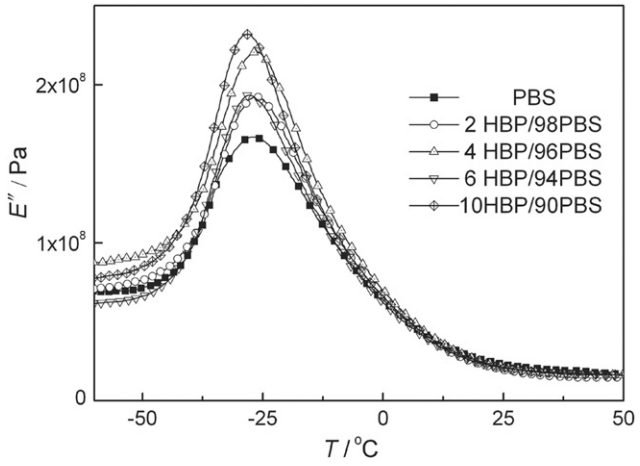

Fig. 13. Curves of E'' vs. T for different samples.

curves are in the viscous region ($G'' > G'$), suggesting that all the flows have more viscous behavior. However, the HBP content obviously influences the viscoelasticity of the melt. When G'' is below 30 Pa, PBS has the lowest viscous behavior, while other blends have more viscous behavior. When G'' is in the range of 30–4000 Pa, the viscous behavior first increases as shown in curve of 2HBP/98PBS, and then decreases with increasing HBP content, indicating that the elastic behavior increases with increasing HBP content. When G'' is larger than 4000 Pa, all of the curves of G' vs. G'' gradually close to the direction of $G' = G''$, suggesting that in the high frequency area, the shear-thinning effect leads to the viscoelasticity of system tending to $G' = G''$ [29].

3.8. Dynamic mechanical analysis

The study on the dynamic mechanical properties of the blends can reveal the changes of the material structure in the process of the temperature increasing and the effect for adding HBP. Figs. 12 and 13 are the curves of the storage modulus (E'), loss modulus (E'') and loss factor (tan δ) of the blends by dynamic temperature scan.

As shown in Fig. 12, the values of E' have the following order within the temperature range from −80 to −50 °C: $E'_{4\%HBP} > E'_{10\%HBP} > E'_{6\%HBP} > E'_{2\%HBP} > E'_{PBS}$, suggesting that each blend at glassy state has larger storage modulus than that of pure PBS because of the influence of the HBP. According to the crystal morphology, tensile strength and rheology behavior of the blends in Figs. 2, 3 and 8, we believe that HBP plays two different roles of a nucleating agent and a plasticizer: (1) When adding a small amount of HBP (2% and 4%), the nucleating agent effect of HBP is dominant, which causes reinforcement and the increased storage modulus, meanwhile the plasticization is not obvious; (2) when adding a large amount of HBP (6% and 10%), apart from some of HBP plays a role of nucleating agent for reinforcement; the others play the apparent role of plasticizer and its effect causes declined storage modulus. However, $E'_{10\%HBP}$ is larger than $E'_{6\%HBP}$, this phenomenon maybe due to the hydrogen bonding between HBP and PBS, which leads to the increase in elastic modulus over the decrease in elastic modulus caused by the plasticization effect.

In addition, as shown in Fig. 12, E' of each sample decreases sharply with temperature increasing from −37.0 to 0 °C. It can also be seen from Fig. 13 that in the vicinity of −25 °C, E'' is on the rise with increasing HBP content in the blend. As seen in Fig. 14, the tan δ peak of pure PBS is at −19.1 °C, while the tan δ peaks of the blends shift slightly to the left along the x-axis with increasing HBP content, especially for the blend with 10%HBP with tan δ peak at −24.2 °C. These results indicate that the glass transition temperature of the blends is decreased with increasing HBP content mainly due to the plasticization effect of HBP. Moreover, the tan δ peak values of PBS and the blends are between 0.1 and 0.12,

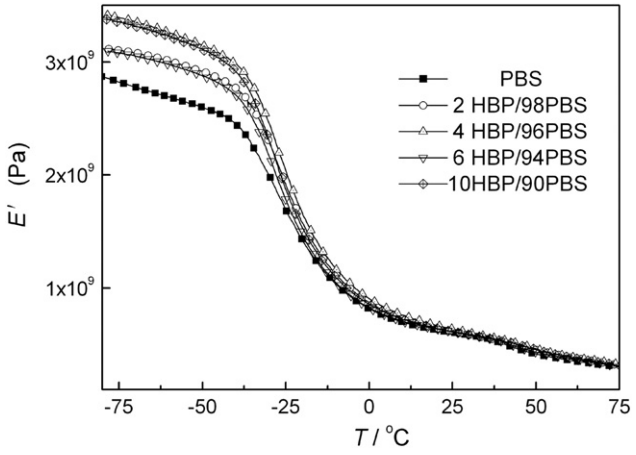

Fig. 12. Curves of E' vs. T for different samples.

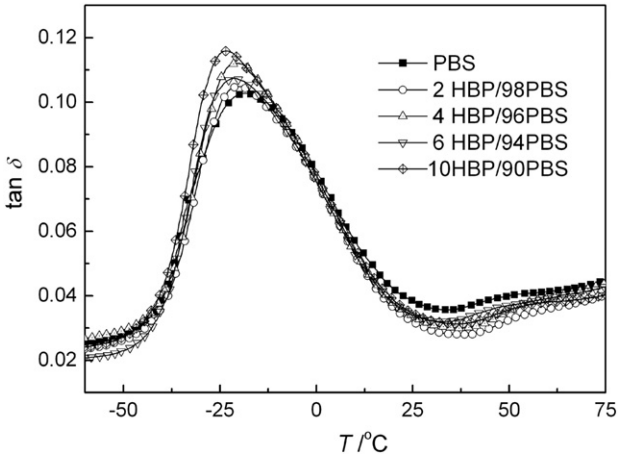

Fig. 14. Curves of tan δ vs. T for different samples.

suggesting that PBS and the blends all have large storage modulus and small loss modulus; but tan δ peak values are gradually increased with increasing HBP content, indicating that the loss modulus and toughness increases slightly due to the plasticization of HBP.

4. Conclusion

In summary, the structure and properties of different PBS/HBP blends were studied by different methods, especially the H-bonding interactions between different molecules. The results of FTIR spectra suggest that a certain number of hydrogen bonds between PBS and HBP is formed, which improves the compatibility between PBS and HBP, and influences the mechanical, rheology and dynamic mechanical properties of the material. HBP phase has a good dispersion in PBS matrix and its phase size increases with increasing HBP content. HBP serves partially as a nucleating agent for the crystallization of PBS, and so the crystallization rate of the blend is increased gradually and the crystal morphology of the blend changes from larger spherulites to microcrystallites. HBP also plays the role of a plasticizer for the blend melt because the complex viscosity of the blends decreases with increasing HBP content, except the blend with 10%HBP because of its abnormal larger complex viscosity at low shear frequencies, which is probably due to the larger H-bonding effect between HBP and PBS. In addition, the melt's elasticity behavior is increased slightly with increasing HBP content. The results of tensile strength, impact strength and storage modulus (the results from the DMA) suggest that proper amount of HBP (4–6%) has a reinforcement effect on the PBS matrix; however, the superfluous HBP can increase the impact strength of the blend mainly due to the plasticization effect or H-bonding effect of HBP on PBS matrix.

Acknowledgment

The authors express their thanks to the financial assistance of the Nature Science Foundation of Hebei Province (the grant no. B2012201112).

Appendix A. Supplementary data

Supplementary data associated with this article can be found in the online version, at http://dx.doi.org/10.1016/j.matchemphys.2013.02.068.

References

[1] H.Y. Li, J. Chang, A.M. Cao, J. Wang, Macromol. Biosci. 5 (2005) 433–440.
[2] M. Giorgio, Paola Rizzarelli, Polym. Degrad. Stab. 70 (2000) 305–314.
[3] H. Nobutaka, S. Ichiro, O. Yoshifumi, JP 045465, 2006.
[4] J.H. Zhao, X.Q. Wang, J. Zeng, G. Yang, F.H. Shi, Q. Yan, Polym. Degrad. Stab. 90 (2005) 173–179.
[5] W.T.S. Anita, J.S. Li, F.T.M. Arthur, Polym. Degrad. Stab. 87 (2005) 487–493.
[6] P.J. Flory VI, J. Am. Chem. Soc. 74 (1952) 2718.
[7] H.R. Kricheldorf, Q.Z. Zang, G. Schwarx, Polymer 23 (1982) 1821–1829.
[8] Y.H. Kim, O.W. Webster, Polym. Prepr. 29 (1988) 310–311.
[9] C.R. Yates, W. Hayes, Eur. Polym. J. 40 (2004) 1257–1281.
[10] Y.H. Kim, O.W. Webster, Macromolecules 25 (1992) 5561–5572.
[11] C. Gao, D. Yan, Chem. Commun. 1 (2001) 107–108.
[12] C. Gao, D. Yan, Macromolecules 34 (2001) 156–161.
[13] J. Zhang, C.P. Hu, Eur. Polym. J. 44 (2008) 3708–3714.
[14] E. Malmstrom, A. Hult, Macromolecules 29 (1996) 1222–1228.
[15] K.L. Wooley, C.J. Hawker, Polym. J. 26 (1994) 187–197.
[16] T.J. Mulkern, N.C. Beck Tan, Polymer 41 (2000) 3193–3203.
[17] R. Mezzenga, C.J.G. Plummer, L. Boogh, J.A.E. Månson, Polymer 42 (2001) 305–317.
[18] D.J. Massa, K.A. Shriner, S.R. Turner, B.I. Voit, Macromolecules 28 (1995) 3214–3220.
[19] O. Monticelli, D. Oliva, S. Russo, C. Clausnitzer, P. Potschke, B. Voit, Mater. Eng. 288 (2003) 318–325.
[20] O. Monticelli, S. Russo, R. Campagna, B. Voit, Polymer 46 (2005) 3597–3606.
[21] S.B. Kil, Y. Augros, Y. Leterrier, J.A.E. Månson, Polym. Eng. Sci. 43 (2003) 329–343.
[22] R. Bhardwaj, A.K. Mohanty, Biomacromolecules 8 (2007) 2476–2484.
[23] J.F. Zhang, X.Z. Sun, Polym. Int. 53 (2004) 716–722.
[24] Y. Li, X.M. Xie, Q. Zong, L.M. Tang, Polymer 46 (2005) 12004–12009.
[25] G. Xu, W.F. Shi, M. Gong, F. Yu, J.P. Feng, Eur. Polym. J. 40 (2004) 483–491.
[26] G. Xu, W.F. Shi, P. Hu, S.P. Mo, Eur. Polym. J. 41 (2005) 1828–1837.
[27] B. Yan, L. Chen, M.F. Zhu, Y.M. Chen, Macromol. Symp. 254 (2007) 167–172.
[28] Y.H. Zhao, Y.Y. Xu, B.K. Zhu, Solid State Ionics 180 (2009) 1517–1522.
[29] Y. Lin, K.Y. Zhang, Z.M. Dong, L.S. Dong, Y.S. Li, Macromolecules 40 (2007) 6257–6267.
[30] D. Lin, W.F. Shi, K.M. Nie, Y.C. Zhang, Polym. Sci. 82 (2001) 1630–1636.
[31] M.M. Coleman, J.F. Graf, P.C. Painter, Technomic, Lancaster, PA, 1991.
[32] M.M. Coleman, P.C. Painter, Prog. Polym. Sci. 20 (1995) 1–59.
[33] Y. He, B. Zhu, Y. Inoue, Prog. Polym. Sci. 29 (2004) 1021–1051.
[34] M. Avrami, J. Chem. Phys. 8 (1939) 212–214.
[35] M. Avrami, J. Chem. Phys. 9 (1941) 177–184.